

Effect of Fiber Type and Coupling Treatment on Properties of High-Density Polyethylene/Natural Fiber Composites

Tian Liu,^a Yong Lei,^b Qingwen Wang,^{a*} Sunyoung Lee,^c and Qinglin Wu^{b,*}

High-density polyethylene (HDPE) and natural fiber composites were prepared by melt compounding and injection molding. The influence of fiber type (*i.e.*, pine, bagasse, rice straw, and rice husk) and the addition of coupling agents on the composite properties were investigated. The use of 30 wt% fiber enhanced the tensile and flexural properties of neat HDPE, but decreased the impact strength. The comprehensive mechanical properties of HDPE/natural fiber composites were significantly improved by the addition of 2 wt% maleated polyethylene (MAPE). The toughness was further enhanced with the use of 5 wt% maleated triblock copolymer styrene-ethylene/butylene-styrene (MASEBS). The composites had higher crystallization peak temperatures and lower crystallinity levels than neat HDPE, and their thermal stability was lower than that of HDPE. The reduced storage modulus and increased loss tangent showed that MASEBS performed as a flexibilizer in composites.

Keywords: Agriculture fiber; Coupling agent; Composites; Plastics; Properties

Contact information: a: Key Laboratory of Bio-based Material Science and Technology (Ministry of Education), Northeast Forestry University, Harbin 150040, China; b: School of Renewable Natural Resources, LSU AgCenter, Baton Rouge, Louisiana; c: Korea Forest Research Institute, Seoul, Korea.
*Corresponding authors: qwu@agcenter.lsu.edu (Qinglin Wu), and qwwang@nefu.edu.cn (Qingwen Wang)

INTRODUCTION

To satisfy the need for a naturally durable wood-based construction material, a new class of composites, known as wood plastic composites (WPCs), has emerged. The WPCs take advantage of low density, low cost, UV resistance, and good machining properties of wood, while the thermoplastic component facilitates flow during melting processes and acts as a barrier layer to retard moisture intrusion and biological attack (Harper and Wolcott 2004).

With increased wood costs and competition for wood resources from traditional wood sectors, developing alternative and environmentally friendly natural fiber sources for plastic composites is greatly needed (Xu *et al.* 2008). These fibers offer many advantages, including high specific strength and modulus, low density, low cost, a renewable nature, easy fiber-surface modification, wide availability, relative abrasion resistance, and the absence of associated health hazards (Faruk *et al.* 2012; Verma *et al.* 2012). Chemically, the organic constituents in natural fibers are mainly cellulose, hemicellulose, and a phenylpropyl structural polymer known as lignin, which are all similar in softwood and hardwood.

Recently, many studies of natural fiber-thermoplastic composites have been carried out that have successfully proven their applicability to various fields of technical

applications. Thermoplastics such as high-density polyethylene (HDPE) (Herrera-Franco and Valadez-Gonzalez 2004; Panthapulakkal and Sain 2007), low-density polyethylene (LDPE) (Georgopoulos *et al.* 2005), polypropylene (PP) (Karmarkar *et al.* 2007; Lopez *et al.* 2012), poly(vinyl chloride) (PVC) (Shah and Matuana 2005; Sombatsompop *et al.* 2003), poly(lactic acid) (PLA) (Huda *et al.* 2006), polystyrene (PS) (Mansour *et al.* 2006), and some recycled thermoplastics (Jayaraman and Bhattacharyya 2004; Lei *et al.* 2007) have been compounded with natural fibers. Furthermore, some natural fibers such as bagasse (Sheshmani 2013), rice straw (Ashori 2013), palm (Abdullah *et al.* 2012), flax (Bledzki *et al.* 2009), and other agroforestry wastes (Hamid *et al.* 2013) have been used as a reinforcement into thermoplastics. However, there is still a large variety of natural fibers that are normally treated as a waste part of the production. Thus, using these natural fibers as a filling material in thermoplastics could be an effective utilization of them and reduce the large amount of waste.

Because the natural fiber component of the composites is hydrophilic and the plastic is hydrophobic, a coupling agent is often used to improve interfacial bonding between the two different phases. Coupling agents function at the interface to create a chemical bridge between the reinforcement and the matrix. Many coupling agents have been investigated and reviewed elsewhere (George *et al.* 2001).

Copolymers containing maleic anhydride, such as maleic anhydride grafted polyethylene (MAPE) or maleic anhydride grafted polypropylene (MAPP), are the most common coupling agents used for natural fiber–thermoplastic composites (Balasuriya *et al.* 2003; Lu *et al.* 2005). The anhydride portion of the MAPE and MAPP can react with a hydroxyl group of the lignocellulose fiber surface and form an ester bond. Meanwhile, the polyethylene segments of MAPE can incorporate themselves into the bulk HDPE matrix. These reactions lead to enhanced physical and mechanical properties of the end products.

In addition to maleated copolymers, some new kinds of coupling agent such as nanoclay (Deka and Maji 2010; Gu *et al.* 2010), polysebacic polyanhydride (PSPA) and polyazelaic polyanhydride (PAPA) (Zhou *et al.* 2010), and m-TMI-g-PP (Li *et al.* 2012) have emerged in recent years. A maleated triblock copolymer styrene-ethylene/butylene-styrene (MASEBS) has also been shown to be an effective impact modifier when used in wood flour and polyolefin systems (Oksman 1996; Oksman and Lindberg 1998). Maleic anhydride is grafted to the ethylene and butylene chain to improve the physical and chemical properties of the polymer by providing polarity to promote hydrophilicity and improve adhesion and compatibility with other polymers and fillers. Several studies using MASEBS as a coupling agent in natural fiber–thermoplastic composite have been published (Kuboki *et al.* 2007; Wang *et al.* 2003). Further work is needed to study the combined effect of MAPE and MASEBS on composite performance.

A direct comparison of fiber performance from various sources under the same processing conditions has rarely been reported, especially under the combined influence of coupling and impact modifying agents. In this study, four kinds of natural fibers, from pine, bagasse, rice straw, and rice husk, were compounded with HDPE. The coupling agent MAPE and the impact modifier MASEBS were used to modify the interface. The objectives of the research were to study the influence of natural fiber type and coupling treatment on the static and dynamic mechanical properties, crystallization behavior, and thermal stability of the HDPE/natural fiber composites.

EXPERIMENTAL

Raw Materials

High-density polyethylene (grade HD6605) with a melt index of 5 g/10 min (190 °C, 2.16 kg) and a density of 0.948 g/cm³ was obtained from ExxonMobil Chemical (Houston, TX, USA).

Pine flour (PF), with particle size passing a 20-mesh screen from American Wood Fibers (Schofield, WI, USA), was used in the experiment as the control. Raw bagasse fiber (BF) was obtained from a local sugar mill in Louisiana. Rice straw (RS) and rice husk (RH) were obtained from the Louisiana State University AgCenter's Crowley Rice Research Station (Crowley, LA, USA). Before being ground, each type of natural fiber was oven-dried at 95 °C for 24 h. The moisture content of the oven-dried material was lower than 2%. The oven-dried material was ground with a Thomas-Wiley miller (Model 3383L10, Swedesboro, NJ, USA) to pass through a 20-mesh screen and then was stored in sealed plastic bags prior to compounding.

MAPE (Polybond 3009, designated MP) with a melt index of 5 g/10 min (190 °C, 2.16 kg) and 1.0 wt% maleic anhydride was obtained from Chemtura (Middlebury, CT, USA). MASEBS (Kraton G1650M, designated MS) with a density of 0.87 g/cm³ and a melt index of less than 1 g/10 min (230 °C, 5 kg) was provided by Kraton (Houston, TX, USA). It has a grafting maleic anhydride level of 1.4 to 2.0 wt% and a styrene/rubber ratio of 30/70 (w/w).

Preparation of HDPE/Natural Fiber Composites

A 1-L thermo-kinetic high-shear mixer (*i.e.*, K-mixer from Synergistics, Quebec, Canada) was used to blend the composites. The raw materials were compounded in the K-mixer at 5000 rpm and discharged when a temperature of 190 °C was reached. The blending was completed in one step for all systems.

The ratio of HDPE and natural fibers was 70:30, wt%. Based on the combined weight of the HDPE and natural fibers, the loading levels of MAPE was 2 wt%. The 5 wt% MASEBS (Xu *et al.* 2008) was added after the compounding of HDPE, natural fibers, and MAPE.

The blends were granulated to pass a 1-cm-opening screen, using a BP68scs granulator (Ball and Jewel, New Berlin, WI, USA). The milled material was then injection-molded at 199 °C with a screw speed of 200 rpm and a mold temperature of 38 °C, using a PLUS injection molder (Wittmann Battenfeld, Kottlingbrunn, Austria).

Measurements and Analysis

Flexural and tensile strength were measured according to ASTM D790-03 and D638-03, respectively, using an INSTRON 5582 Testing Machine (Instron, Grove City, PA, USA). A TINIUS 92T impact tester (Testing Machine, Horsham, PA, USA) was used for the Izod impact test. All samples were notched at the center point of one longitudinal side according to ASTM D256. For each treatment level, five replications were tested.

Wide-angle X-ray diffraction (XRD) analysis was carried out with a MiniFlex diffractometer (Rigaku, Tokyo, Japan) to investigate the change of crystalline thickness of HDPE in the composites. XRD samples were taken from compression-molded specimens and were mounted to the XRD platform for analysis. Scattered radiation was

detected in a 2θ range from 5° to 35° at $5^\circ/\text{min}$ in reflection mode. A computer-controlled wide-angle goniometer coupled to a sealed-tube source of Cu $K\alpha$ radiation ($\lambda = 1.54056 \text{ \AA}$) was used. The Cu $K\alpha$ was filtered electronically with a thin Ni filter. The crystalline thickness perpendicular to the reflection plane was calculated using the Scherrer formula (Patterson 1939) with an instrument width of 0.16° . The crystalline thickness perpendicular to the reflection plane (L_{hkl}) can be calculated as

$$L_{hkl} = \frac{K\lambda}{\beta \cos \theta} \quad (1)$$

$$\beta_0^2 = \beta_M^2 - \beta_I^2 \quad (2)$$

where β is the increment of the diffraction beam, β_0 is the width of the diffraction beam (rad), β_M is the measured width of the diffraction beam (rad), β_I is the instrument width (rad), and K is the shape factor of crystalline thickness, related to β_0 and L_{hkl} . When β_0 is defined as the half-height width of diffraction peaks, $K = 0.9$.

The crystallization behavior of HDPE in the composites was further explored using a differential scanning calorimeter (DSC Q100, TA Instruments, New Castle, DE, USA). Samples of 5 to 8 mg were placed in aluminum capsules and heated from 40 to 160°C at the rate of $10^\circ\text{C}/\text{min}$ to eliminate the heat history before cooling at $10^\circ\text{C}/\text{min}$. The crystalline level (X_t) of the HDPE matrix was evaluated from the following relationship,

$$X_t = \frac{\Delta H_{\text{exp}}}{\Delta H} \times \frac{1}{W_f} \times 100\% \quad (3)$$

where ΔH_{exp} is the experimental heat of fusion or crystallization determined from DSC, ΔH is the assumed heat of fusion or crystallization of fully crystalline HDPE, taken as 276 J/g as previously reported (Lepers *et al.* 1997), and W_f is the weight fraction of HDPE in the composites. For each treatment level, three replications were tested.

Thermogravimetric analysis (TGA) was used to study the thermal stability characteristics of the composites with a thermogravimetric analyzer (Q50, TA Instruments, New Castle, DE, USA), under nitrogen at a scan rate of $10^\circ\text{C}/\text{min}$ from room temperature to 650°C . A sample of 5 to 8 mg was used for each run. For each treatment level, three replications were tested.

Dynamic mechanical analysis (DMA) of the composites was performed with a dynamic mechanical analyzer (Q800, TA Instruments, New Castle, DE, USA). The tests were performed in dual cantilever mode at a frequency of 1 Hz at a heating rate of $1^\circ\text{C}/\text{min}$. Before each test, the samples ($60 \text{ mm} \times 10 \text{ mm} \times 3 \text{ mm}$) were conditioned for 72 h at a temperature of 23°C and a relative humidity of 50%. For each treatment level, three replications were tested.

The morphology of the composites was studied with a Hitachi VP-SEM S-3600N (Hitachi, Tokyo, Japan) scanning electron microscope. The fracture surfaces of the specimens after the impact test were sputter-coated with gold before analysis.

RESULTS AND DISCUSSION

Static Mechanical Properties of Composites

Table 1 shows the static mechanical properties of composites containing different natural fibers and coupling agents. The four kinds of composites exhibited similar trends in static mechanical properties. For each composite, flexural and tensile modulus and flexural strength increased significantly with natural fibers added, while impact strength decreased remarkably, especially for the HDPE/bagasse fiber composite. This indicates that natural fibers performed as a stiff reinforcement in composites and that the plastic matrix provided toughness. Based on data shown in Table 1, natural fiber types showed a distinct influence on each mechanical property, especially flexural and tensile moduli. Compared with the HDPE/pine fiber composites, the HDPE/bagasse fiber composite showed the highest flexural and tensile properties but the lowest impact strength.

Table 1. Static Mechanical Properties of HDPE and Its Composites with Various Fibers

System*	Flexural		Tensile		Impact Strength (kJ/m ²)
	Strength (MPa)	Modulus (GPa)	Strength (MPa)	Modulus (GPa)	
HDPE	21.7 (0.9) g	0.64 (0.06) j	17.0 (0.2) i	0.37 (0.01) i	12.7 (0.28) a
HDPE/PF	31.6 (1.0) ef	1.52 (0.06) c	18.1 (0.3) h	1.95 (0.13) b	4.66 (0.22) ef
HDPE/BF	39.3 (0.5) b	1.90 (0.05) a	18.6 (0.2) g	2.23 (0.09) a	3.87 (0.27) g
HDPE/RS	29.9 (2.3) f	1.30 (0.02) de	16.2 (0.2) j	1.70 (0.08) d	4.40 (0.17) f
HDPE/RH	30.5 (2.1) f	1.27 (0.06) ef	15.2 (0.1) k	1.36 (0.03) fg	4.76 (0.21) de
HDPE/PF/MP	40.7 (1.3) b	1.35 (0.04) d	22.9 (0.3) b	1.84 (0.11) c	4.74 (0.21) de
HDPE/BF/MP	45.4 (1.8) a	1.67 (0.11) b	26.0 (0.1) a	2.04 (0.15) b	5.00 (0.43) d
HDPE/RS/MP	37.0 (1.1) c	1.28 (0.03) ef	21.7 (0.5) d	1.70 (0.04) d	3.97 (0.19) g
HDPE/RH/MP	35.2 (0.3) cd	1.14 (0.05) h	21.2 (0.2) e	1.29 (0.11) g	4.55 (0.20) ef
HDPE/PF/MP+MS	36.0 (1.9) cd	1.20 (0.05) gh	19.4 (0.3) f	1.50 (0.03) e	5.72 (0.20) c
HDPE/BF/MP+MS	39.7 (0.3) b	1.33 (0.02) de	22.6 (0.1) c	1.64 (0.09) d	5.76 (0.23) c
HDPE/RS/MP+MS	35.0 (1.2) d	1.23 (0.05) fg	19.4 (0.2) f	1.41 (0.10) ef	4.77 (0.19) de
HDPE/RH/MP+MS	32.9 (0.9) e	0.97 (0.02) i	18.5 (0.2) g	1.11 (0.10) h	6.34 (0.27) b

* The weight ratio of HDPE and natural fiber in the composites was 70:30. MAPE and MASEBS concentrations were 2% and 5% based on the total weight of HDPE and natural fiber, respectively. The values in the parentheses are standard deviations. For a property in the same list, means with the same letter for the property are not significantly different at the 5% significance level based on Duncan's multiple range test.

In the presence of MAPE, much improved flexural and tensile strengths were observed for all the composites, compared with the corresponding composites without MAPE. In most wood plastic composites, the flexural properties depend largely on the distribution of fiber in the matrix and the tensile properties are more sensitive to interfacial interactions between the two main phases (Balasuriya *et al.* 2001). The improvement in flexural and tensile strength due to the addition of MAPE may be attributed to the increased interfacial compatibility. However, the flexural and tensile modulus of the composites showed an opposite trend to that of strength when MAPE was

added. Modulus is a parameter characterizing the ability of materials to prevent stress-induced deformation. It was anticipated that the hydrophilic anhydride groups that were more compatible with natural fibers would not only improve the adhesion between the two main interfaces but also promote the dispersion of natural fibers in the composites. Hence, the composites should be more flexible because of the homogeneous mixing between the two phases. Moreover, further improvement in impact strength was found with the presence of MASEBS, especially in the HDPE/rice husk system, which exhibited an improvement of 39.3% in impact strength. Meanwhile, a slight reduction in flexural and tensile properties was exhibited due to the elastomeric nature of MASEBS.

Effect of Natural Fibers and Coupling Agents on HDPE Crystallization

X-ray diffractograms of HDPE and its composites are presented in Fig. 1a, and Fig. 1b shows X-ray diffractograms of the HDPE/rice straw system with an added coupling agent. The DSC cooling curves of HDPE and HDPE/natural fiber composites are shown in Fig. 2. The diffraction peaks for the (110) and (200) planes of HDPE shifted little when the natural fibers and coupling agent were added, suggesting that the dimensions of the polyethylene cell did not change. However, a significant reduction in the diffraction peak intensity was observed with the presence of natural fibers, suggesting that there was an increased disordering after natural fibers were added.

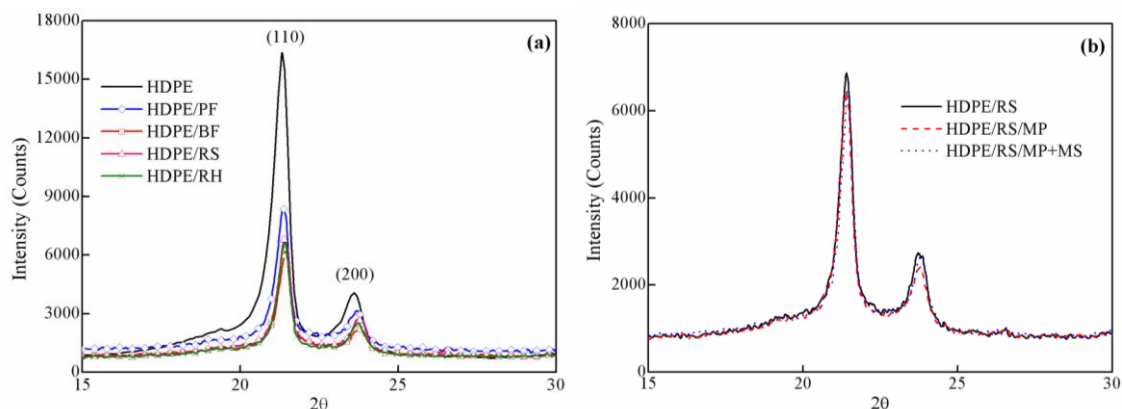


Fig. 1. XRD patterns for 2θ angles of 15 to 30° of (a) HDPE and HDPE/natural fibers composites and (b) the HDPE/rice straw system with coupling agent added

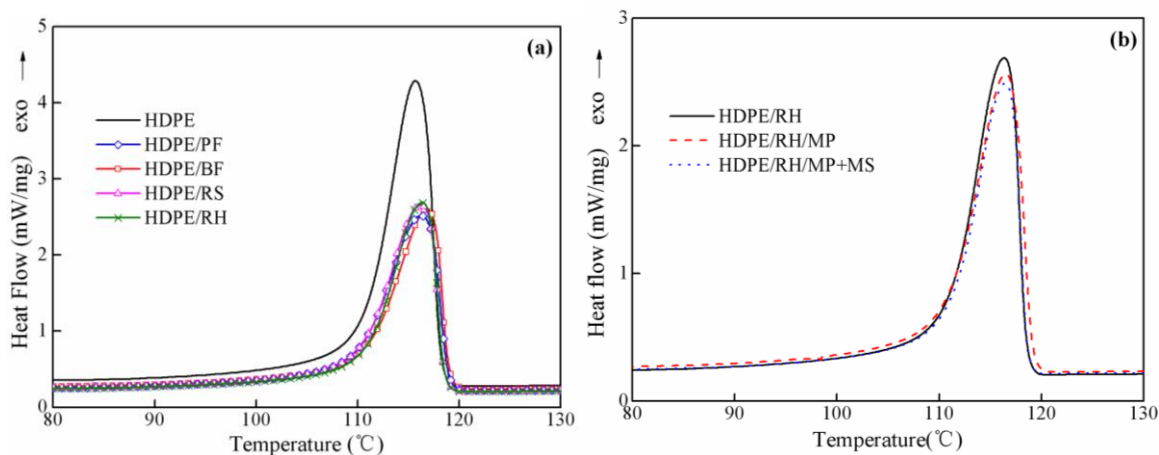


Fig. 2. DSC cooling curves of (a) HDPE and HDPE/natural fibers composites and (b) the HDPE/rice husk system with a coupling agent added at a cooling rate of $10^\circ\text{C}/\text{min}$ in N_2

The crystalline thickness from XRD tests and the crystallization entropy and crystalline content from DSC are shown in Table 2. The values of L_{hkl} of neat HDPE were 16.0 nm for the (110) plane and 13.9 nm for the (200) plane. The crystallization temperature of neat HDPE was 115.7 °C, and its X_t was 52.3%. The addition of 30 wt% natural fiber increased the values of L_{hkl} for both the (110) plane and the (200) plane, slightly increased the crystallization temperature, and significantly decreased ΔH_{exp} of the composites (Fig. 2a). It could be expected that natural fibers would certainly increase the matrix viscosity at the crystallization temperature and would reduce the diffusion rate of the chain of polyethylene. The increase of L_{hkl} might result from that reason and also from the crystal imperfection of natural fibers. Moreover, the natural fibers not only had no nucleate effects, but they also mildly inhibited the crystallization of the HDPE matrix, which can be deduced from the fact that the X_t in the composites was lowered.

Table 2. Crystalline Thickness of HDPE from XRD and Crystalline Levels from DSC

System*	Crystalline Thickness (nm)		Crystallization Enthalpy (J/g)	Crystalline Level X_t (%)
	L110	L200		
HDPE	16.0	13.9	144.3	52.3
HDPE/PF	17.4	16.1	97.8	50.3
HDPE/BF	17.6	14.2	93.7	48.5
HDPE/RS	17.5	14.7	97.2	50.3
HDPE/RH	18.6	16.8	92.9	48.1
HDPE/PF/MP	17.1	15.2	101.8	53.7
HDPE/BF/MP	18.0	17.1	91.1	48.1
HDPE/RS/MP	17.8	15.8	88.9	46.9
HDPE/RH/MP	18.4	15.4	90.0	47.5
HDPE/PF/MP+MS	17.6	15.9	102.7	56.9
HDPE/BF/MP+MS	18.1	15.9	88.2	48.8
HDPE/RS/MP+MS	18.2	15.3	85.3	47.2
HDPE/RH/MP+MS	18.6	16.2	84.4	46.7

* The weight ratio of HDPE and natural fiber in the composites was 70:30. MAPE and MASEBS concentrations were 2% and 5%, respectively, based on the total weight of HDPE and natural fiber.

With the addition of MAPE and MASEBS, the crystallization peak barely changed in both the XRD (Fig. 1b) and DSC results (Fig. 2b). For HDPE/bagasse fiber, rice straw, and rice husk composites, the same trend of reduced crystallization level was obtained with the addition of the coupling agent (Table 2), which could be attributed to the improved interfacial interaction between the natural fiber and the HDPE matrix. The mobility of HDPE became limited, and a part of the HDPE in the composite would be fixed against its crystallization. For HDPE/pine flour composites, the addition of 2 wt% MAPE decreased the value of L_{hkl} for both the (110) and (200) plane and increased the X_t of the composite, but it did not influence the peak position, while 5% MASEBS increased the L_{hkl} and further increased the X_t , in contrast to the other composites.

Thermogravimetric Behavior of HDPE/Natural Fiber Composites

The thermogravimetric analysis parameters are summarized in Table 3. Typical TGA and DTG curves are shown in Figs. 3 and 4, respectively. There were two degradation peaks for the composites containing natural fibers. The first peak appeared at about 332 to 369 °C from the degradation of natural fiber, and the other appeared at about 480 °C as a result of the HDPE decomposition (Fig. 3a). The degradation onset point of composites containing four different natural fibers differed significantly, as did the Peak I temperature, possibly because the four natural fibers have different thermogravimetric behaviors. As shown in Fig. 3b, the natural fibers slightly increased the peak temperature of HDPE. This suggests that the large size of natural fibers may limit the melt flow of polymer and restrict its rearrangement due to steric hindrance; hence, the peak of HDPE moved toward the right (Yao *et al.* 2007). This may also explain the slight increase in the crystallization peak temperature of HDPE/natural fiber composites (Fig. 2a). The residual weight of HDPE/rice straw and HDPE/rice husk composites was about 11% due to the ash content in rice straw and rice husk.

Table 3. Thermal Degradation Temperature and Residual Weight of HDPE and Its Composites

System ¹	Onset Point ² (°C)	Peak Temp ³ (°C)		Residue (%)
		Peak I	Peak II	
HDPE	444.7	-	471.1	0.7
HDPE/PF	288.4	368.7	483.9	4.5
HDPE/BF	272.6	358.4	481.5	8.4
HDPE/RS	251.6	332.4	482.8	11.5
HDPE/RH	266.4	353.8	479.0	11.8
HDPE/BF/MP	272.6	358.4	482.9	8.1
HDPE/BF/MP+MS	273.1	357.4	481.2	7.6

¹ The weight ratio of HDPE and natural fiber in the composites was 70:30. MAPE and MASEBS concentrations were 2% and 5%, respectively, based on the total weight of HDPE and natural fibers.
² Initial thermal degradation temperature
³ The peak temperature of the weight derivative curves

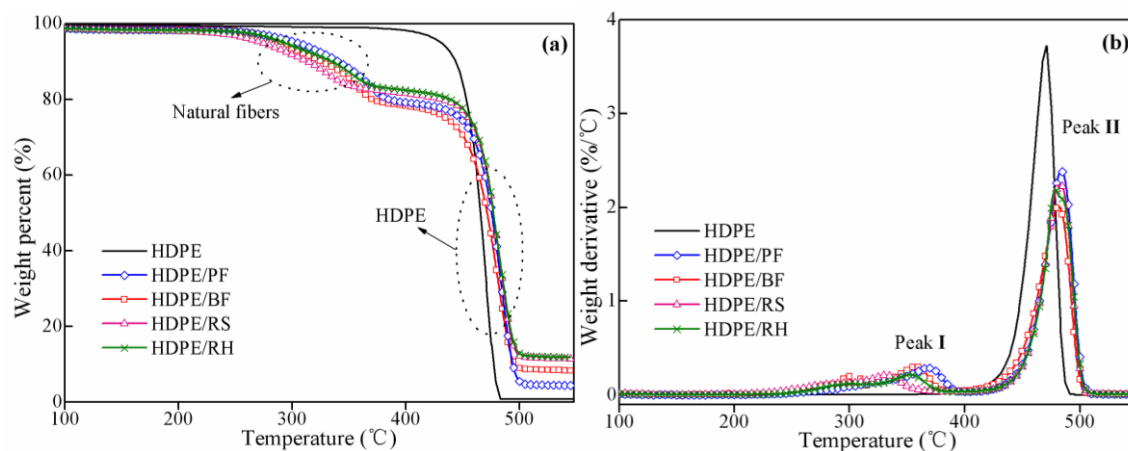


Fig. 3. Temperature dependence of (a) weight loss and (b) its first derivative with respect to temperature for HDPE and its composites at 10 °C/min in N₂

As shown in Fig. 4 and Table 3, the addition of the coupling agents MAPE and MASEBS had little influence on the decomposition behavior of HDPE/bagasse fiber composites.

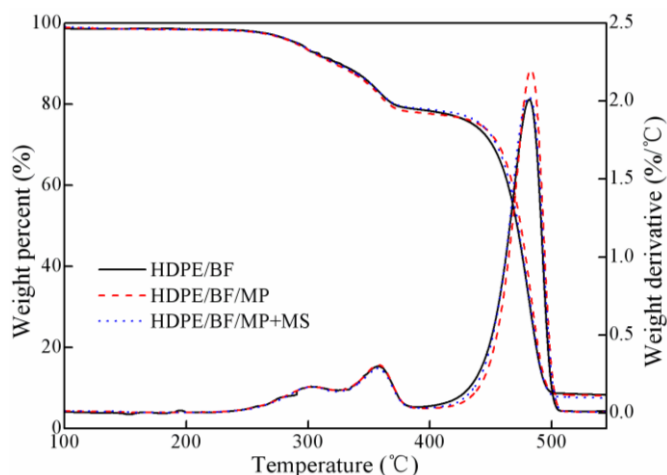


Fig. 4. Temperature dependence of weight loss and its first derivative with respect to temperature for the HDPE/bagasse fiber system at 10 °C/min in N₂

Dynamic Mechanical Analysis

Figure 5 shows the storage modulus (G') and loss tangent ($\tan\delta$) versus temperature for neat HDPE and filled HDPE composites. A considerable improvement in G' was seen with the addition of the fibers. The effect was more obvious for the HDPE/pine flour composites, and the other three fiber systems (*i.e.*, BF, RH, and RS) showed much similar behavior (data for RS not shown in Fig. 5). $\tan\delta$ is a parameter that expresses the differences in viscoelastic response of the materials and is independent of the materials' stiffness (Tajvidi *et al.* 2006). The wide peak of $\tan\delta$ at about 100 °C found for HDPE mainly resulted from the α -transition of polyethylene (Simon *et al.* 2001). This peak became less apparent when 30 wt% fibers were added. Meanwhile, a decrease in $\tan\delta$ height was observed. Pure HDPE showed the highest $\tan\delta$ value over the entire temperature range due to decreases in the volume fraction of the matrix with the incorporation of natural fibers (Deka *et al.* 2011; Jiang and Kamdem 2008).

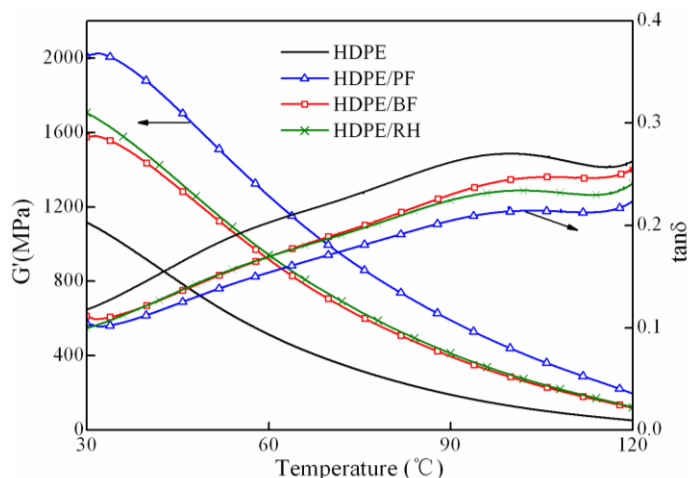


Fig. 5. DMA curves showing storage modulus (G') and loss tangent ($\tan\delta$) for HDPE and composites containing natural fibers at a heating rate of 1 °C/min

Figure 6 shows the storage modulus (G') and loss tangent ($\tan\delta$) versus temperature for the HDPE/pine flour system with a coupling agent. There are only slight differences in both G' and $\tan\delta$ at low temperature with the addition of MAPE. When the MASEBS was introduced, the composite showed higher $\tan\delta$ and lower G' than the others did, over most of the temperature range. This indicates that MASEBS performed as a flexibilizer in the composites; hence, $\tan\delta$, which characterizes the viscoelastic response of materials, increased, and G' , which represents the stiffness of the materials, decreased. This is also in support of the static mechanical properties of the composites with the addition of MASEBS (Table 1).

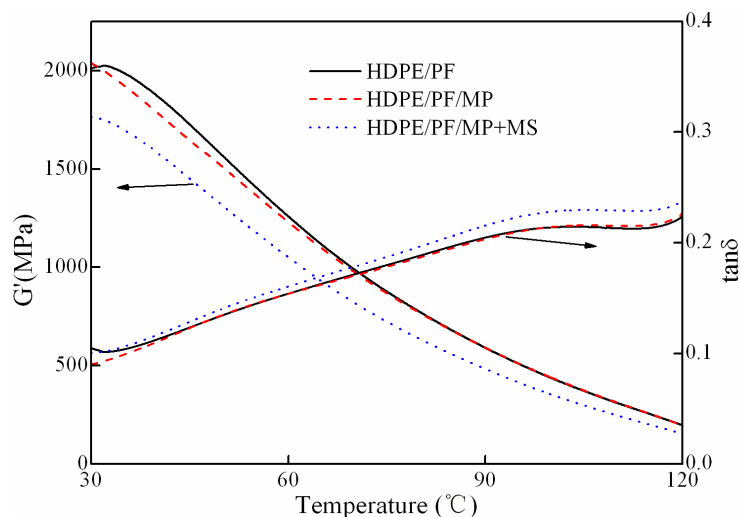


Fig. 6. DMA curves showing the coupling agent effect on the storage modulus (G') and the loss tangent ($\tan\delta$) for the HDPE/pine flour system at a heating rate of 1 °C/min

Fracture Morphology Analysis

The fractured surfaces of the HDPE/bagasse fiber composites are presented in Fig. 7. Without coupling agents, there was obvious separation between HDPE and the fibers, and the interface between them was clear (Fig. 7a), indicating the incompatibility between the hydrophobic matrix and the hydrophilic natural fibers. With the addition of MAPE, some fractured fibers appeared in the composite and the matrix was better bonded to the fibers (Fig. 7b), suggesting that the fractures of the fiber itself rather than debonding were the main energy dissipation mode in this case. Hence, the interfacial adhesion between the HDPE and the fibers was remarkably improved by MAPE.

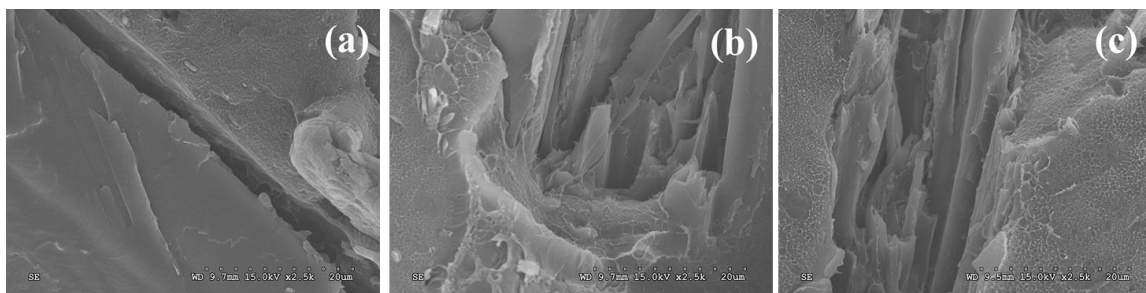


Fig. 7. SEM micrographs of the impact fracture surface of HDPE/bagasse fiber composites containing (a) no coupling agents; (b) 2 wt% MAPE; and (c) 2 wt% MAPE and 5 wt% MASEBS

The interfacial compatibility between the filler and plastic matrix can dominantly determine the shear strength between the two phases and accordingly the mechanical properties of the composites. This may explain the better flexural and tensile properties achieved for the composites containing MAPE. When MAPE was coupled with MASEBS as combined coupling agents, the interfacial boundary became indistinct and the breakage of fibers was not observed, as shown in Fig. 7c. The matrix deformation around the fillers became more pervasive, which was consistent with the highest impact strength among these composites.

CONCLUSIONS

1. The four kinds of natural fiber-based composites studied exhibited similar trends in static mechanical properties. The 30 wt% natural fiber improved the mechanical properties of neat HDPE, except for impact strength. The comprehensive mechanical properties of HDPE/natural fiber composites were significantly improved with 2 wt% MAPE, and the toughness was further enhanced with 5 wt% MASEBS.
2. The crystallization peak temperature of HDPE slightly increased when the natural fibers were introduced, but it hardly changed with the coupling agent. The natural fiber also increased the values of L_{hkl} and decreased the crystallinity levels of composites. For composites based on bagasse, rice straw, and rice husk, the coupling agent lowered the crystallization enthalpy and the crystallinity levels.
3. The TGA onset point and peak temperature varied with each of the fiber types of natural fiber-based composites. The coupling agents had little influence on thermal degradation.
4. The natural fibers lowered the value of $\tan\delta$ and improved G' compared with neat HDPE. The reduced G' and increased $\tan\delta$ showed that MASEBS performed as a flexibilizer in composites.

ACKNOWLEDGMENT

This research was financially supported by the National Natural Science Foundation of China (Grant No. 31010103905) and by the Korea Forest Research Institute. The authors would like to thank Dr. Craig Clemens at the USDA Forest Products Laboratory in Madison, WI, for his generous support in preparing test samples.

REFERENCES CITED

- Abdullah, C. K., Jawaid, M., Khalil, H. P. S. A., Zaidon, A., and Hadiyane, A. (2012). "Oil palm trunk polymer composites: Morphology, water absorption, and thickness swelling behaviors," *BioResources* 7(3), 2948-2959.
- Ashori, A. (2013). "Effects of nanoparticles on the mechanical properties of rice straw/polypropylene composites," *J Compos Mater.* 47(2), 149-154.

- Balasuriya, P., Ye, L., and Mai, Y. W. (2001). "Mechanical properties of wood flake-polyethylene composites. Part I: Effects of processing methods and matrix melt flow behaviour," *Compos. Pt. A-Appl. Sci. Manuf.* 32(5), 619-629.
- Balasuriya, P. W., Ye, L., and Mai, Y. W. (2003). "Morphology and mechanical properties of reconstituted wood board waste-polyethylene composites," *Compos. Interfaces.* 10(2-3), 319-341.
- Bledzki, A. K., Lucka, M., Al Mamun, A., and Michalski, J. (2009). "Biological and electrical resistance of acetylated flax fibre reinforced polypropylene composites," *BioResources* 4(1), 111-125.
- Deka, B. K., and Maji, T. K. (2010). "Effect of coupling agent and nanoclay on properties of HDPE, LDPE, PP, PVC blend and *Phargamites karka* nanocomposite," *Compos. Sci. Technol.* 70(12), 1755-1761
- Deka, B. K., Maji, T. K., and Mandal, M. (2011). "Study on properties of nanocomposites based on HDPE, LDPE, PP, PVC, wood and clay," *Polym. Bull.* 67, 1875-1892.
- Georgopoulos, S. T., Tarantili, P. A., Avgerinos, E., Andreopoulos, A. G., and Koukios, E. G. (2005). "Thermoplastic polymers reinforced with fibrous agricultural residues," *Polym. Degrad. Stab.* 90(2), 303-312.
- Faruk, O., Bledzki, A. K., Fink, H. P., and Sain, M. (2012). "Biocomposites reinforced with natural fibers: 2000-2010," *Prog. Polym. Sci.* 37(11), 1552-1596.
- Gu, R., Kokta, B. V., Michalkova, D., Dimzoski, B., Fortelny, I., Slouf, M., and Krulis, Z. (2010). "Characteristics of wood-plastic composites reinforced with organo-nanoclays," *J. Reinf. Plast. Compos.* 29(24), 3566-3586.
- Hamid, Y., Abu Bakar, A., and Deirram, N. (2013). "Mechanical and morphological properties of waste *Eurycoma longifolia* fiber/montmorillonite reinforced poly(vinyl chloride) hybrid composites," *J. Appl. Polym. Sci.* 128(2), 1170-1175.
- Harper, D., and Wolcott, M. (2004). "Interaction between coupling agent and lubricants in wood-polypropylene composites," *Compos. Pt. A-Appl. Sci. Manuf.* 35(3), 385-394.
- Herrera-Franco, P.J., and Valadez-Gonzalez, A. (2004). "Mechanical properties of continuous natural fibre-reinforced polymer composites," *Compos. Pt. A-Appl. Sci. Manuf.* 35(3), 339-345.
- Huda, M. S., Drzal, L. T., Mohanty, A. K., and Misra, M. (2006). "Chopped glass and recycled newspaper as reinforcement fibers in injection molded poly(lactic acid) (PLA) composites: A comparative study," *Compos. Sci. and Technol.* 66(11-12), 1813-1824.
- Jayaraman, K., and Bhattacharyya, D. (2004). "Mechanical performance of woodfibre-waste plastic composite materials," *Resour. Conser. Recy.* 41(4), 307-319.
- Jiang, H. H., and Kamdem, D. P. (2008). "Thermal and dynamic mechanical behavior of poly (vinyl chloride)/wood flour composites," *J. Appl. Polym. Sci.* 107(2), 951-957.
- Karmarkar, A., Chauhan, S. S., Modak, J. M., and Chanda, M. (2007). "Mechanical properties of wood-fiber reinforced polypropylene composites: Effect of a novel compatibilizer with isocyanate functional group," *Compos. Pt. A-Appl. Sci. Manuf.* 38(2), 227-233.
- Kuboki, T., Lee, Y. H., Park, C. B., and Sain, M. (2007). "Effects of styrene-ethylene-butylene-styrene based additives on the mechanical properties of rice hull/polypropylene composites," *Polym. Eng. Sci.* 47(7), 1148-1155.

- Lei, Y., Wu, Q., Yao, F., and Xu, Y. (2007). "Preparation and properties of recycled HDPE/natural fiber composites," *Compos. Pt. A-Appl. Sci. Manuf* 38(7), 1664-1674.
- Lepers, J. C., Favis, B. D., and Tabar, R. J. (1997). "The relative role of coalescence and interfacial tension in controlling dispersed phase size reduction during the compatibilization of polyethylene terephthalate/polypropylene blends," *J. Polym. Sci. Pt. B: Polym. Phys.* 35(14), 2271-2280.
- Li, L., Wang, Q., and Guo, C. (2012). "The influence of wood flour and compatibilizer (m-TMI-g-PP) on crystallization and melting behavior of polypropylene," *J. Therm. Anal. Calorim.* 107(2), 717-723.
- Lopez, J. P., Girones, J., Mendez, J. A., El Mansouri, N. E., Llop, M., Mutje, P., and Vilaseca, F. (2012). "Stone-ground wood pulp-reinforced polypropylene composites: Water uptake and thermal properties," *BioResources* 7(4), 5478-5487.
- Lu, J., Wu, Q., and Negulescu, I. I. (2005). "Wood-fiber/high-density-polyethylene composites: Coupling agent performance," *J. Appl. Polym. Sci.* 96(1), 93-102.
- Mansour, S. H., El-Nashar, D. E., and Abd-El-Messieh, S. L. (2006). "Effect of chemical treatment of wood flour on the properties of styrene butadiene rubber/polystyrene composites," *J. Appl. Polym. Sci.* 102(6), 5861-5870.
- Oksman, K. (1996). "Improved interaction between wood and synthetic polymers in wood/polymer composites," *Wood Sci. Technol.* 30(3), 197-205.
- Oksman, K., and Lindberg, H. (1998). "Influence of thermoplastic elastomers on adhesion in polyethylene wood flour composites," *J. Appl. Polym. Sci.* 68(11), 1845-1855.
- Panthapulakkal, S., and Sain, M. (2007). "Agro-residue reinforced high-density polyethylene composites: Fiber characterization and analysis of composite properties," *Compos. Pt. A-Appl. Sci. Manuf.* 38(6), 1445-1454.
- Patterson, A. (1939). "The Scherrer formula for X-ray particle size determination," *Phys. Rev.* 56(10), 978.
- Shah, H. L., and Matuana, L. M. (2005). "Novel coupling agents for PVC/wood-flour composites," *J. Vinyl Addit. Technol.* 11(4), 160-165.
- Sheshmani, S. (2013). "Effects of extractives on some properties of bagasse/high density polypropylene composite," *Carbohydr. Polym.* 94(1), 461-419.
- Simon, L., De Souza, R., Soares, J., and Mauler, R. (2001). "Effect of molecular structure on dynamic mechanical properties of polyethylene obtained with nickel-diimine catalysts," *Polym.* 42(11), 4885-4892.
- Sombatsompop, N., Chaochanchaikul, K., Phromchirasuk, C., and Thongsang, S. (2003). "Effect of wood sawdust content on rheological and structural changes, and thermo-mechanical properties of PVC/sawdust composites," *Polym. Int.* 52(12), 1847-1855.
- Tajvidi, M., Falk, R. H., and Hermanson, J. C. (2006). "Effect of natural fibers on thermal and mechanical properties of natural fiber polypropylene composites studied by dynamic mechanical analysis," *J. Appl. Polym. Sci.* 101(6), 4341-4349.
- Verma, D., Gope, P. C., Maheshwari, M. K., and Sharma, R. K. (2012). "Bagasse fiber composites – A review," *J. Mater. Environ. Sci.* 3(6), 1079-1092.
- Wang, Y., Yeh, F. C., Lai, S. M., Chan, H. C., and Shen, H. F. (2003). "Effectiveness of functionalized polyolefins as compatibilizers for polyethylene/wood flour composites," *Polym. Eng. Sci.* 43(4), 933-945.
- Xu, Y., Wu, Q., Lei, Y., Yao, F., and Zhang, Q. (2008). "Natural fiber reinforced poly(vinyl chloride) composites: Effect of fiber type and impact modifier," *J. Polym. Environ.* 16(4), 250-257.

- Yao, F., Wu, Q., Lei, Y., Guo, W., and Xu, Y. (2007). "Thermal decomposition kinetics of natural fibers: Activation energy with dynamic thermogravimetric analysis," *Polym. Degrad. Stab.* 93(1), 90-98.
- Zhou, J., Sheng, J., Wang, Y., Xu, Y., and Yang, H. (2010). "Interface research of wood/plastic composites modified by long chain segment block graft," *Rare. Metal. Mater. Eng.* 39(2), 390-393.

Article submitted: May 13, 2013; Peer review completed: June 17, 2013; Revised version received and accepted: July 22, 2013; Published: July 24, 2013.